Structural and optical properties of the M@C_{59}X cages (X=N, B and M=Li, Na)

MOJTABA YAGHOBI[1,*] and ALIREZA ADABINEZHAD[2]

[1] Ayatollah Amoli Branch, Islamic Azad University, Amol, Iran
[2] Science and Research Branch, Islamic Azad University, Mazandaran, Iran
*Corresponding author. E-mail: m.yaghoubi@iauamol.ac.ir

Abstract. Using B3LYP/6-31G* density functional level of theory, the structural and optical properties of the C_{60} and M@C_{59}X cages have been investigated. Results indicate that the charge on C atoms and band gap of C_{60} cage are changed dramatically with the substitution of one B or N atom at one of the C sites and the Li and Na atom encapsulations in the C_{60} cage. The Mulliken analyses show that the charge is transferred completely between the alkali atoms and the C_{59}X cage. The substitutional and encapsulation doping (SED) reduce the optical gaps of the C_{60} cage. Also, the oscillator strengths of the absorption peaks are dependent on dopant types.

Keywords. *Ab initio*; doping; cage; absorption; electronic structure.

PACS Nos 31.15.−A; 33.15.−E; 33.15.Fm; 81.07.Nb

1. Introduction

After the discovery of 60-atom clusters and large carbon-cage molecules [1–6], the studies of nanostructured materials based on the family of fullerene molecules have attracted the attention of scientists and materials scientists [1–6]. Fullerenes are closed hollow cages of carbon atoms interconnected in pentagonal and hexagonal rings. Derivations of all the basic fullerenes such as C_{70}, C_{76} and C_{84} are possible. Soon after the discovery of fullerenes, endohedral metallofullerenes, fullerenes with encapsulated metal atoms and substitute doping (SD), i.e., substituting one or more carbon atoms of fullerenes by other atoms, were obtained [7–9]. Fullerenes doped with alkali, alkaline earth and lanthanide metal atoms are of great interest in both experimental and theoretical studies of new types of chemical species. The C_{59}N or C_{59}B heterofullerenes were predicted to provide a doping opportunity for C_{60} [10,11]. In general, heterofullerenes possess a rich chemistry due to their enhanced reactivity as compared to pristine fullerenes [11]. The C_{59}N

azafullerene can be synthesized in macroscopic amounts [11,12]. Endohedral molecules of $M@C_{60}$ with M = N, P, Li, Ca, Na, K, Rb can be prepared by a 'brute force' method in small quantities [13]. The studies indicated that a low-energy surface is generated for the flow of M atom when ion moves from the centre of the $M@C_{60}$ cage towards minimum energy and the charge is transferred to the carbon cage of $M@C_{60}$. Overall, the geometric structures, symmetric properties, the highest occupied molecular orbitals (HOMO), lowest unoccupied molecular orbitals (LUMO) and the electronic polarization of fullerenes are varied greatly due to the doping effect [11–15].

There is limited information on the possibility that heterofullerenes could encapsulate other atoms or molecules. Hou and Kang investigated the relative stabilities of all isomers of $Sc_3N@C_{67}B$, $Sc_3N@C_{67}N$ and $Sc_3N@C_{66}BN$ using density functional theory. The calculations predicted that $Sc_3N@C_{68}$ can be doped substitutionally in a much better way with a boron atom than C_{60} [16]. The endohedral fullerenes encapsulating trimetallic nitride clusters, $Er_xSc_{3-x}N@C_{80}$ ($x = 0$–3), were produced using small amounts of nitrogen in an electric-arc reactor [17]. Dorn *et al* have found that the Sc_3N moiety is encapsulated in a highly symmetric, icosahedral C_{80} cage, which is stabilized as a result of charge transfer between the nitride cluster and the fullerene cage [17]. $Y_2@C_{79}N$ and $Y_2@C_{79}N$ were obtained by performing the Krätschmer–Huffman electric arcprocess [18]. The unpaired electron of $Y_2@C_{79}N$ is localized in a bonding orbital between the two yttrium ions of this stable radical. The dimetallic endohedral heterofullerenes (EHF), $Gd_2@C_{79}N$, was prepared and isolated in a relatively high yield. Computational (DFT), chemical reactivity, Raman and electrochemical studies all suggested that the purified $Gd_2@C_{79}N$, with the heterofullerene cage, $(C_{79}N)^{5-}$ has comparable stability with other better known isoelectronic metallofullerene $(C_{80})^{6-}$ cage species (e.g., $Gd_3N@C_{80}$) [19,20].

The pure and doped fullerenes have many applications and are extremely useful in military, medical field, nanotechnology and many other fields because they are extremely resilient, sturdy, quite stable chemically and physically, have highest tensile strength of any known 2D structure or element, highest packing density of all known structures and are impenetrable to all elements under normal circumstances [7,8,20–28].

The spintronics and optoelectronics depend on finding and utilizing new semiconductors to keep the fullerenes moving forward. Therefore, the electronic and geometric structures of new materials are of basic interest to understand the material formation and properties. In this paper, we investigate the structural and optical properties of the heterofullerenes (substituting one carbon atom with a boron or nitrogen atom) which encapsulate other Li and Na atoms.

2. Computational details

Figure 1 shows the fully optimized geometry of $Li@C_{59}B$ by using the Gaussian 98 program [29]. The B3LYP/6-31G method was useful for studying the large cages and different nanostructures [16–20,30,31]. The minimum total potential energy of endohedral complexes was determined by full geometry optimization using B3LYP/6-31G* method. The optical properties of the C_{60} and $M@C_{59}X$ cages were theoretically studied using perturbation theory [32,33].
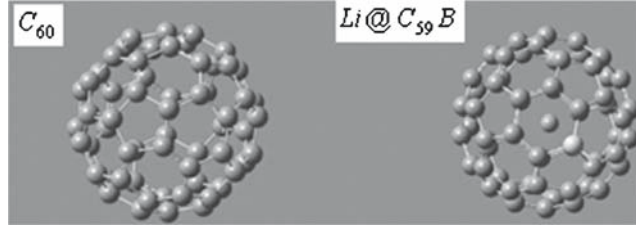
Figure 1. The optimized structure of the C$_{60}$ and Li@C$_{59}$B cages.

The dynamic polarizabilities were calculated by TDDFT-B3LYP/6-31G*.

The first-order polarizability can be determined from the energy change using the following equation [33]:

$$\alpha_{ij}(-\omega; \omega) = \sum_{p \neq 0} \frac{\langle 0| \hat{\mu}_i |p\rangle \langle p| \hat{\mu}_j |0\rangle}{(\omega_p - \omega - i\gamma)} + \sum_{p \neq 0} \frac{\langle 0| \hat{\mu}_i |p\rangle \langle p| \hat{\mu}_j |0\rangle}{(\omega_p + \omega + i\gamma)}, \quad (1)$$

where p denotes the excited state and 0, the ground state; μ_j is the j $(= x, y, z)$th component of the dipole; $(h/2\pi)\omega_p$ is the transition energy between the p and 0 states and γ $(= 0.016$ eV) is the Lorentzian distribution width.

The eigenvalues (ω_p) and eigenstates in eq. (1) are obtained by diagonalizing an eigenvalue problem involving the effective two-particle Hamiltonian [34]:

$$H_{(n_1,n_2),(n_3,n_4)} = (\varepsilon_{n_2} - \varepsilon_{n_1})^2 \delta_{n_1,n_3} \delta_{n_2,n_4} + H'_{(n_1,n_2),(n_3,n_4)}.$$

Here, $(\varepsilon_{n_2} - \varepsilon_{n_1})$ is the transition energy which is obtained with respect to the one-electron energy (ε_n) of TDDFT-B3LYP/6-31G*. For simplicity, we consider $H'_{(n_1,n_2),(n_3,n_4)} = 0$ in the calculations.

3. Results and discussion

In this study, the effect of the substitutional and encapsulation doping (SED) on the structural and optical properties of the C$_{60}$ cage has been investigated at the B3LYP/6-31G* density functional level of theory. The optimized structures of the C$_{60}$ and M@C$_{59}$X cages are shown in figures 1a–1c. As shown in figure 1a, C$_{60}$ fullerene consists of 20 hexagonal and 12 pentagonal faces with 60 carbon atoms located at the vertices of regular truncated icosahedrons of I_h symmetry. Each carbon atom is bonded to three others and is sp_2 hybridized.

The ground-state level diagrams near the Fermi level of the C$_{60}$ and M@C$_{59}$X cages are shown in figure 2. It should be mentioned that energy levels with differences between each other being less than 0.01 eV are arranged as degenerate. The R^{Max} and R^{Min} values of bond lengths, LUMO–HOMO gaps and total energy E_T of C$_{60}$ and M@C$_{59}$X cages are listed in table 1. Results indicate that all degeneracies are lifted when M and X atoms are doped in the C$_{60}$ cage. For example, the LUMO and HOMO of C$_{60}$ consist of three
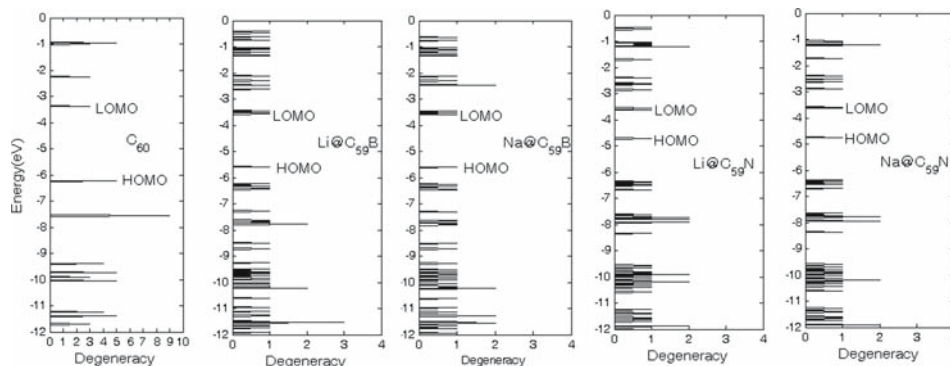
Figure 2. The energy level diagrams of the C_{60}, Li@C_{59}B, Li@C_{59}N, Na@C_{59}B and Na@C_{59} N cages.

and five degenerate orbitals, respectively. But, these have one degenerate orbital for the M@C_{59}X cages. The degeneracy is almost always related to symmetry and it is lifted due to the reduction in symmetry. The LUMO energy value of the C_{60} molecule is about the same as that of the M@C_{59}X cages. Also, the HOMO of C_{60} molecule is lower in energy than HOMOs of M@C_{59}X cages.

The C–C bond lengths are experimentally determined to be 1.450 and 1.387 Å. In excellent agreement with experiment [35], C=C and C–C bond lengths of C_{60} molecule are 1.384 Å and 1.464 Å, respectively. Results indicate that maximum change in bond lengths ($\Delta R^{\text{Max}} = R^{\text{Max}} - R^{\text{Min}}$) is related to the M@$C_{59}$B cages. The bond lengths vary from 1.39 to 1.47 Å and 1.38 to 1.55 Å for the Na@C_{59}N and M@C_{59}B cages, respectively. All B–C bonds of the M@C_{59}B cage are considerably longer than C–C bonds of the C_{60} and M@C_{59}X cages and N–C bonds of M@C_{59}N cage. Also, maximum change in C–C bond lengths ($= R_{\text{CC}}^{\text{Max}} - R_{\text{CC}}^{\text{Min}}$) of M@$C_{59}$X cages is more than that of C_{60} cage.

After X and M doping, a hole is doped in the HOMO of the C_{60} cage, and empty level is split from the occupied level, so that the LUMO– HOMO gap of C_{60} cage is reduced. The band gap of the C_{60} cage decreases greatly by the N and X doping. Therefore, M@C_{59}X cages are expected to be more reactive than the C_{60} cage. Also, the M@C_{59}N cages

Table 1. The maximum (R^{Max}) and minimum (R^{Min}) values of the bond lengths for carbon–carbon (C–C), boron–carbon (B–C) and carbon–nitrite (N–C) (in Å), the LUMO–HOMO gap (E_{g} in eV) and the total energy (E_{T} in a.u.) of the C_{60}, Li@C_{59}B, Li@C_{59} N, Na@C_{59}B and Na@C_{59}N cages.

	$R_{\text{CC}}^{\text{Min}}$	$R_{\text{CC}}^{\text{Max}}$	$R_{\text{BC}}^{\text{Min}}$	$R_{\text{BC}}^{\text{Max}}$	$R_{\text{NC}}^{\text{Min}}$	$R_{\text{NC}}^{\text{Max}}$	E_{g}	E_{T}
C_{60}	1.34	1.44	–	–	–	–	2.873	−225.5
Li@C_{59}N	1.394	1.474	–	–	1.431	1.442	1.103	−2309.70
Na@C_{59}N	1.394	1.475	–	–	1.431	1.442	1.101	−244.49
Li@C_{59}B	1.39	1.47	1.494	1.554	–	–	2.02	−2279.7
Na@C_{59}B	1.39	1.47	1.494	1.554	–	–	2.029	−2434.0

Table 2. The positions and distance of the M (Li and Na) and X (B and N) atoms relative to the cage centre of the C$_{60}$, Li@C$_{59}$B, Li@C$_{59}$N, Na@C$_{59}$B and Na@C$_{59}$N cages. Here $r = \sqrt{(x^2 + y^2 + z^2)}$ and x, y and z are in Cartesian coordinates.

	Li@C$_{59}$N		Na@C$_{59}$N		Li@C$_{59}$B		Na@C$_{59}$B	
	N	Li	N	Na	B	Li	B	Na
x	0.35	0.00	0.34	0.00	3.741	0.00	3.744	0.00
y	−3.538	0.00	−3.537	−0.097	3.343	0.00	−0.327	0.00
z	−0.002	0.00	0.003	0.00	−0.039	0.00	0.0072	0.00
r	3.555	0.00	3.554	0.097	3.7557	0.00	3.7599	0.00

possess much smaller gaps compared to the M@C$_{59}$B cages. The M@C$_{59}$B cages possess much larger gaps compared to the M@C$_{59}$N cages. Depending on the dopant types, the band gaps of the M@C$_{59}$X cages change from 1.01 to 2.029 eV. For doped molecules, the smallest band gap is related to the Na@C$_{59}$N cage and the highest band gap is related to the Na@C$_{59}$B cage. Thus, the M@C$_{59}$X cages can be used to produce semiconductors with various band gaps. For the M@C$_{59}$X cages, it is clear that the effect of X-doped atom type on the band gap is more than the effect of M-doped atom type. This is because Li and Na atoms belong to the same groups of chemical elements, but, N and B atoms belong to different groups of chemical elements.

In table 1, it can be observed that the abstract values of the total energies for M@C$_{59}$N and Na@C$_{59}$B(Li@C$_{59}$B) increase(decrease) with the replacement of X and M atoms on the C$_{60}$ cage. Also, Li@C$_{59}$X and C$_{60}$ molecules have nearly the same total energy, showing that they are almost equally stable.

In table 2, we present the positions of M and X atoms relative to the centre of the cages. Interestingly, the results suggest that the Na atom resides off-centre of the Na@C$_{59}$N molecule. Therefore, it reaches a minimum energy that is lower than the energy at the centre of the cage when the Na atom moves a certain distance from the centre of the cage. Results show that minimum energy positions of Na and Li in the Na@C$_{59}$B and Li@C$_{59}$X molecules are at the centre of cage.

The distance of the X atom from the centre of the cage increases with respect to the type of the substituted atom. The distance of the B atom from the centre of the M@C$_{59}$B molecules is larger than the distance of N atom from the centre of the M@C$_{59}$N molecules which is independent of the M-doped atom type. Overall, the results indicate that the C$_{60}$ cage symmetry breaks by M and X doping.

The net Mulliken charges (Q_i) of M@C$_{59}$X molecules are presented in table 3. The sign of atomic charge can be appraised correctly by the Mulliken analysis, but it cannot exactly predict the atomic charges quantitatively [36].

The results show that the endoatoms can act as electronic donors due to the large positive charges of Na and Li atoms. Therefore, we can assume that the charge is transferred completely between the alkali atom and the C$_{59}$X cage.

For the M@C$_{59}$B cages, the Mulliken analyses show that carbon atoms have negative Q_i and the B atom has positive Q_i. Therefore, the boron atom in M@C$_{59}$B acts as electron donor while carbon atoms act as electron acceptors. The experimental result by the Smalley group [8] says that an electron-deficient site was produced at the boron position on the cage. Then, the calculated charge of boron atom is consistent with the experimental result [37].

Table 3. The Mulliken charges of the M (Li and Na) and X (B and N) atoms and the nearest-neighbour C atoms of the X atom of the Li@C_{59}B, Li@C_{59}N, Na@C_{59}B and Na@C_{59}N cages.

	Q_x	Q_M	Q_1	Q_2	Q_3
Li@C_{59}N	−0.0	1.041	0.214	0.215	0.207
Na@C_{59}N	−0.3	0.909	0.209	0.21	0.21
Li@C_{59}B	0.191	1.03	0.00	−0.077	−0.077
Na@C_{59}B	0.199	0.901	0.00	−0.078	−0.078

Although the charges of the nearest-neighbour C atoms of the N atom for the M@C_{59}N molecules are positive, the other charges of the C atoms are negative. Therefore, the nearest-neighbour C atoms of the N atom in M@C_{59}N exist as electron donors while other carbon atoms and N atom act as electron acceptors.

The optical absorption (imaginary part of first-order polarizability) dispersions of the C_{60} and M@C_{59}B cages are calculated and the spectra are averaged over three orientations. Average data are displayed in figures 3, 4a, 4b, 4c and 4d for C_{60}, Li@C_{59}B, Li@C_{59}N, Na@C_{59}B and Na@C_{59}N cages respectively. The optical gaps of the M@C_{59}B cages are equal to the band gaps between HOMO and LUMO of the M@C_{59}B cages with a weak absorption peak. Therefore, the optical gap becomes smaller by replacing one C atom with one B or N atom and encapsulating one Li or Na atom on C_{60}.

After the SED, the oscillator strengths of absorption peaks of the C_{60} cage decreases. Also, the number of peaks of C_{60} cage increases by SED. The maximum value of absorption peaks of the M@C_{59}B cages is larger than that of the M@C_{59}N cages. We propose the following explanation for these behaviours. It is clear that absorption spectrum is dependent on two factors, namely, the transition energy and transition matrix element between one-electron states. Also, the symmetric property of the cage affects transition matrixes. Overall, the effects of degeneracy of energy levels, band gap and symmetric properties of the cage are important in absorption spectrum. The distortion of cage structure and changes in bond lengths are due to SED. It is evident that cage structure
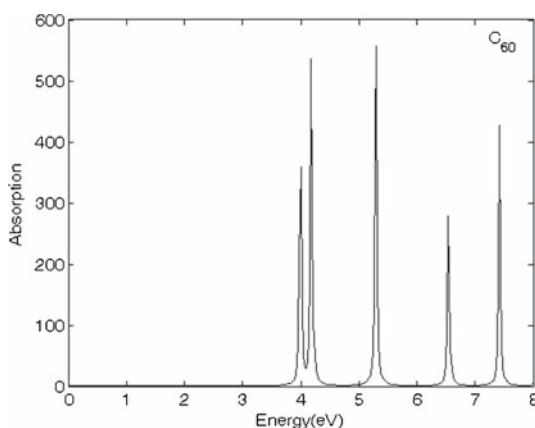
Figure 3. The absorption spectra of the C_{60} cage.
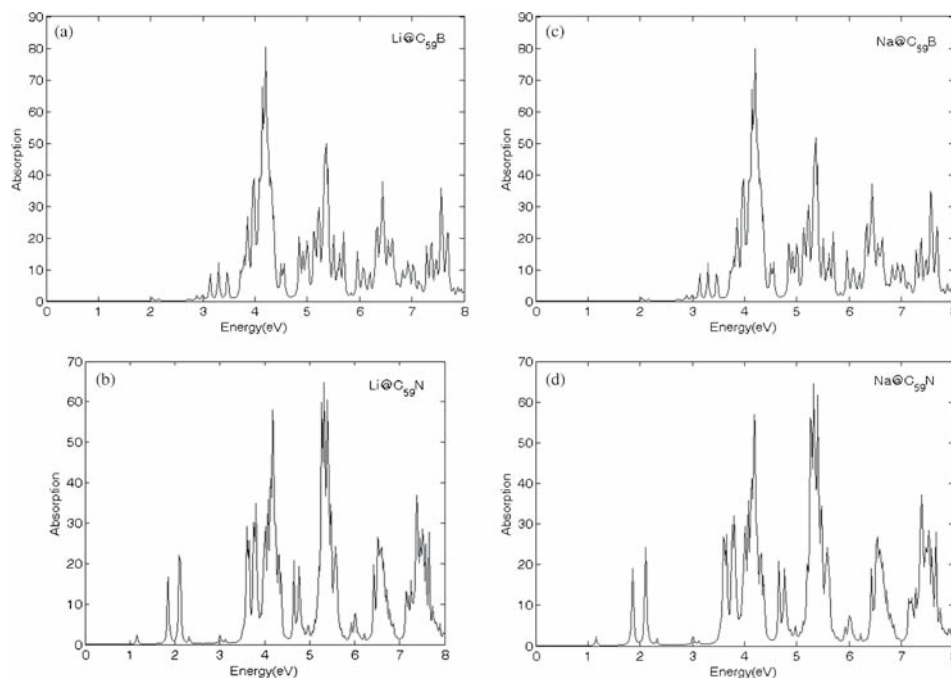
Figure 4. The absorption spectra of (**a**) Li@C$_{59}$B, (**b**) Li@C$_{59}$N, (**c**) Na@C$_{59}$B and (**d**) Na@C$_{59}$N cages.

and symmetric properties are dependent on the SED types. That is, SED breaks the cage symmetry and thus changes the electronic structures and absorption spectra of the C$_{60}$ cage.

4. Conclusions

Effects of encapsulation and substitutional doping on the structural and optical properties of the C$_{60}$ cages were studied using the B3LYP/6-31G* level of density functional theory. By replacing one C atom with one N and B atom and Li and Na atoms encapsulation on the C$_{60}$ cage, the structural and symmetric properties, optical absorption spectra and band gap of the C$_{60}$ cages are changed. The Mulliken analyses showed that carbon atoms in M@C$_{59}$B have negative charge and the charges of nearest-neighbour C atoms of N atom in the M@C$_{59}$N molecules are positive. Our calculations concluded that M@C$_{59}$X cages can be interesting candidates for application in optoelectronics and spintronics.

References

[1] H W Kroto, J R Heath, S C O'Brien, R F Curl and R E Smalley, *Nature* **318**, 162 (1985)
[2] K Jinno, H Matsui, H Ohta, Y Saito, K Nakagawa, H Nagashima and K Itoh, *Chromatographia* **41**, 353 (1995)
[3] K Jinno, T Uemura, H Ohta, H Nagashima and K Itoh, *Anal. Chem.* **65**, 2650 (1993)
[4] W Krätschmer, L D Lamb, K Fostiropoulos and D R Huffman, *Nature* **347**, 354 (1990)

[5] H Ajie, M M Alvarez, S J Anz, R D Beck, F Diederich, K Fostiropoulos, D R Huffman, W Kraetschmer, Y Rubin, K E Schriver, D Sensharma and R Whetten, *J. Phys. Chem. B* **94**, 8630 (1990)

[6] F Diederich, R Ettl, Y Rubin, R L Whetten, R Beck, M Alvarez, S Anz, D Sensharma, F Wudl, K C Khemani and A Koch, *Science* **252**, 548 (1991)

[7] J R Heath, S C O'Brien, Q Zhang, Y Liu, R F Curl, F K Tittel and R E Smalley, *J. Am. Chem. Soc.* **107**, 7779 (1985)

[8] Y Chai, T Guo, C Jin, R E Haufler, L P F Chibante, J Fure, L Wang, J M Alford and R E Smalley, *J. Phys. Chem.* **95**, 7564 (1991)

[9] R D Johnson, M S de Vries, J R Salem, D S Bethunde and C S Yannoni, *Nature* **355**, 239 (1992)

[10] W Andreoni, F Gygi and M Parrinello, *Chem. Phys. Lett.* **190**, 159 (1992)

[11] J C Hummelen, C Bellavia-Lund and F Wudl, *Heterofullerenes in topics in current chemistry* (Springer, Berlin, Heidelberg, 1999)

[12] J C Hummelen, B Knight, J Pavlovich, R Gonzalez and F Wudl, *Science* **269**, 1554 (1995)

[13] L Forro1 and L Mihaly, *Rep. Prog. Phys.* **64**, 649 (2001)

[14] F Langa and J-F Nierengarten (Eds) *Fullerenes: Principles and applications* (Thomas Graham House, Cambridge, 2007)

[15] M S Dresselhaus, G Dresselhaus and P C Eklund, *Science of fullerenes and carbon nanotubes: Their properties and applications* (Academic Press, New York, 1996)

[16] J Q Hou and H S Kang, *J. Phys. Chem. A* **111**, 1111 (2007)

[17] S Stevenson *et al*, *Nature* **401**, 55 (1999)

[18] T Zuo, L Xu, C M Beavers, M M Olmstead, W Fu, T D Crawford, A L Balch and H C Dorn, *J. Am. Chem. Soc.* **130**, 12992 (2008)

[19] W Fu *et al*, *Am. Chem. Soc.* **133**, 9741 (2011)

[20] Y Ma, T Wang, J Wu, Y Feng, Li Jiang, C Shuand and C Wang, *Chem. Commun.* **48**, 11570 (2012)

[21] D M Guldi and N Martin, *Fullerenes: From synthesis to optoelectronic properties* (Kluwer Academic Publisher, Dordrecht, The Netherlands, 2002)

[22] E Osawa, *Perspectives in fullerene nanotechnology* (Springer, Berlin, Germany, 2002)

[23] Y Kim, S Cook, S M Tuladhar, S A Choulis, J Nelson, J R Durrant, D D C Bradley, M Giles, I Mcculloch, C S Ha and M Ree, *Nat. Mater.* **5**, 197 (2006)

[24] N Burangulov, A P Moravsky, Y V Kulikova, R O Loutfy and G I Dyachuk, *Cosmetic compositions containing fullerene clusters*, Patent US 5612021 (2006)

[25] W Wilson, International Center for Scholars, Project on emerging nanotechnologies (2007)

[26] N Tagmatarchis and H Shinohara, *Mini-Rev. Med. Chem.* **1**, 339 (2001)

[27] S G Kim and D Tomzinek, *Phys. Rev. Lett.* **72**, 2418 (1994)

[28] V Buntar and H W Weber, *Supercond. Sci. Technol*. **9**, 599 (1996)

[29] Gaussian 98, Revision A 9, M J Frisch *et al*, Gaussian, Inc, Pittsburgh PA, 1998

[30] P Karamanis and C Pouchan, *Int. J. Quantum Chem.* **111**, 788 (2011)
P Karamanis, R Marchal, P Carbonniére and C Pouchan, *J. Chem. Phys.* **135**, 044511 (2011)

[31] W J Hehre, R Ditchfield and J A Pople, *J. Chem. Phys.* **56**, 2257 (1972)

[32] R D Mattuck, *A guide to Feynman diagrams in the many-body problem* (McGraw-Hill, New York, 1967)

[33] B J Orr and J F Ward, *Mol. Phys.* **l20**, 513 (1971)

[34] W Guan, C G Liu, P Song, G C Yang and Z M Su, *Theor. Chem. Acc.* **122**, 265 (2009)
S J A van Gisbergen, J G Snijders and E J Baerends, *Comput. Phys. Commun.* **118**, 119 (1999)

[35] H B Bürgi, E Blanc, D Schwarzenbach, S Liu, Y Lu, M M Kappes and J A Ibers, *Angew. Chem. Int. Ed*(*Engl.*) **41**, 640 (1992)

[36] A Szabo and N S Ostlund, *Modern quantum chemistry* (Macmillan, New York, 1982)

[37] T Guo, C M Jin and R E Smalley, *J. Phys. Chem.* **95**, 4948 (1991)